applied sciences

MDPI

Article

Design and Structural Validation of a Device for Assisted Vehicle Boarding

Albert Mareš [1], Peter Malega [1,*], Naqib Daneshjo [2], Zuzana Štofková [3] and Tomáš Mišenčík [4]

[1] Faculty of Mechanical Engineering, Technical University of Kosice, 042 00 Kosice, Slovakia; albert.mares@tuke.sk
[2] Faculty of Commerce, Bratislava University of Economics and Business, 852 35 Bratislava, Slovakia; daneshjo47@gmail.com
[3] Faculty of Operation and Economics of Transport and Communications, University of Zilina, 010 26 Zilina, Slovakia; zuzana.stofkova@uniza.sk
[4] Iveco Czech Republic, a. s., Čelakovského 271, 566 01 Vysoké Mýto, Czech Republic; tomasmisencik20@gmail.com
* Correspondence: peter.malega@tuke.sk; Tel.: +421-55-602-3236

Abstract

Population aging increases the demand for different assistive devices enabling independent mobility and safe vehicle boarding. This paper presents the design and development of a universal lifting platform intended to support the legs of people with reduced mobility during vehicle entry. The device was designed to be independent of a specific vehicle and to be powered by vehicle standard 12 Volt current. A CAD model of the proposed device was modeled in SolidWorks 2017 and validated through analytical calculations and finite element simulations. Based on the calculation results, a functional prototype was manufactured and tested under real operating conditions, confirming the feasibility and usability of the proposed solution. The presented platform provides a low-cost, lightweight and vehicle-independent assistive device, supporting controlled and safe leg transfer without the need for vehicle modification or homologation.

Keywords: assistive device; vehicle boarding; lifting platform; finite element analysis; power screw

1. Introduction

Population aging represents a contemporary trend and, at the same time, a significant challenge for society. The process of population aging is described using forecasts derived from demographic indicators, each of which demonstrates an increasing tendency within the time frame up to 2060. These data were published by the Institute of Informatics and Statistics of the Slovak Republic. In addition, EUROSTAT also reports a continuing increase in the population age structure, where the age group of 65 years old and over increases in the EU from 19.1% in year 2015 to 22% in year 2025, and the estimation to the year 2060 is increasing to 30% of the population [1]. Based on projections prepared by several independent institutions, a substantial aging of the population is anticipated. Along with a rising average age, there is an increase in the prevalence of illnesses, including disorders of the musculoskeletal system.

Given this trend of an increasing average age, it is essential to consider the need to ensure the mobility of individuals who often experience significantly reduced mobility. For this reason, it is necessary to focus on the development of devices that can maintain

Received: 11 February 2026
Revised: 26 March 2026
Accepted: 30 March 2026
Published: 17 April 2026

people's mobility and independence for as long as possible. In the development of such devices, it is crucial to determine the appropriate functional requirements, which must be preceded by the identification of the types of individuals for whom the aid is intended. Each type of individual requires an aid with specific characteristics, reflecting the nature of their reduced mobility.

Along with the increasing average age, there is a corresponding rise in morbidity, the need for care, as well as the necessity to provide mobility for individuals with partially or completely restricted movement. In view of this fact, it is essential to address the issue of ensuring mobility for people in higher age groups. To provide mobility, it is necessary to develop various aids and devices that enable the maintenance of self-sufficiency and the highest possible level of independence from the assistance of others. Many authors, teams and companies are focused on developing such aid because of the increasing number of older people and thus the increasing market potential for such aids. In [2–7], it is possible to see different approaches to such aid development, including using biomechanical principles [8], virtual reality [9], and augmented reality [10], and exploring mobility patterns [11] using video [12], autonomous robots [13], etc. Moreover, there are studies about the behavior of elderly people, which helps with understanding their needs [14,15] and then adapting services and products to their needs. In addition, there are approaches that use mobility aids to investigate the mobility of people with diseases [16] and systems for path planning [17].

As demonstrated, there is crucial interest in looking for ways to improve the life of elderly people and people with some disabilities. Because of their decreasing health, elderly people usually need some kind of transport. Very often, it is a passenger car, and for some people, they have problems getting into the car. One problem is that the car seat is on a lower level, and the other problem is getting the legs into the car. There are some aids that can help to make the sitting-to-stand transition and vice versa easier [18], but the problem is that some of these devices are not suitable to use to sit in the car (there is no space for them, or it is not possible to adjust the device correctly).

When developing such aids, it is crucial to determine the specific type of user for whom the device is intended, and to adapt the design accordingly to ensure the simplest possible operation while fulfilling all necessary functions, given the considerably limited space available for installation. These aids can also be classified according to the degree of intervention required in the vehicle's construction. For some aids, only minor or no modifications are necessary, whereas others require significant intervention in the vehicle structure, which must be approved by the relevant homologation authority. The target is developing a device that will help get the legs into the car without the need for homologation. These devices are called leg lifters.

As a result of these considerations, this article is devoted to the design and calculation of an aid that, through its functionality, facilitates boarding and alighting from a vehicle by lifting and repositioning the legs of a person with partial mobility impairment. For this activity, it is necessary that the process of lifting be controlled by the person for whom the aid is intended, as only the individual concerned knows to what extent leg elevation can be performed without pain. If operated by another person, manipulation could potentially cause pain or even injury to the affected individual. An important factor in the design is the universality and a construction that is independent of the vehicle, thereby eliminating the need for homologation of the technical fitness of the vehicle and reducing the overall cost of the aid. Universality ensures applicability to the widest possible range and types of vehicles.

According to the literature and web resources, there are many institutions and companies considering using leg lifters to put the legs into the car, as mentioned in [19,20].

There are some types of leg lifters, e.g., Turny Evo, which was presented as a swivel-and-lowering car seat. This solution allows the seat to rotate out of the vehicle and lower to wheelchair height, which makes transferring into the car much easier for people with reduced mobility [21].

In 2015, the patent "Leg Lifter" (US20150351992A1) described a simple leg-lifting aid. This device helps a user lift their leg, including when getting into a car, and is especially useful for people with limited lower-limb mobility [22].

Very similar to the previous solution is the Ansa Leg Lifter, which "enables user to move an immobile leg when transferring or dressing, enables small loop fits around hand or wrist and large stiffened loop slides over foot or shoe and provides control in lifting and lowering the leg" [23].

Another solution called the "Car Leg Lifter" is presented and described in [24].

Turny Evo offers the highest level of support for people with leg problems, but it requires car construction adoption. Other solutions are based on a simple piece of canvas or rope with a foot loop and handle to lift and reposition the legs. This solution is simple, cheap and easy to carry, but is not suitable for all people. There are people with specific mobility problems. Some people need to change the position of legs while lifting them up. That means they lift the legs a little bit up, then they need adjust the joints (knee and hips), then they continue to lift the legs and then again they need to stop lifting the legs, again adjust the joints and then continue. When adjusting the joints, they need support for the legs, and they cannot hold a handle on the above-mentioned leg lifter and simultaneously adjust the joints, because it requires a lot of effort. Moreover, when other people want to help them, it is a problem because of pain. When another person grasps their legs and manipulates them, it can cause great pain to the person, because an assisting person cannot accurately detect the onset of pain experienced by the user. When pain occurs, it may be necessary to lower the legs slightly, reposition them laterally, and then continue the transfer in a controlled stepwise manner. The only person who knows precisely what is necessary to do is the person whose legs are lifted.

Based on the information above, it is possible to state that there is no device that can help people in the way mentioned in the previous paragraph. Accordingly, the decision was taken to design such a device.

2. Materials and Methods

Based on the information above, the specifications for a leg lifter were defined:

- Lifter should support legs during the whole time necessary to move legs into the car.
- Lifter should be able to stop at any time during lifting.
- Lifter should be able to move down any time after stopping lifting.
- Movement up and down must be controlled by the person whose legs are lifted.
- Lifter should be lightweight and easily removable.
- Lifter should be possible to use with nearly any passenger car.
- Lifter should be powered by energy standardly accessible in the passenger car (most common is electric power with voltage 12 V).
- Lifter size should be such that it will be possible to transport it in the passenger car.

To design the leg lifter, the following methods and materials were used:

- Distance measurement to determine maximum height of lifting.
- Calculation of maximum loads to determine maximum load.
- CAD modeling to create 3D model of leg lifter.
- Matrix calculations.
- FEM analysis to determine stress and displacement in leg lifter construction.
- Prototype production and testing to evaluate results of calculations.

2.1. Maximum Height of Lifting

When using the device for boarding, it is important that the user's legs, once lifted, are aligned with the upper edge of the car door sill, which is covered by a protective plastic trim. This trim represents the height to which the platform must be raised, together with the legs of the person with limited mobility. The movement to this height must be smooth and stable, with secure fixation of the feet to prevent slipping.

This height was determined by measuring the relevant distances on real vehicles of various classes and brands. Collected data are in Table 1. It shows recorded distances to the lower edge of the car door sill—representing the shortest distance between the ground and the vehicle—and to the upper plastic trim, which defines the required lifting height.

Table 1. Values of car door sill distances from ground.

Vehicle Brand	Distance to Lower Edge of Car Door Sill (cm)	Distance to Upper Plastic Edge of Car Door Sill (cm)
Fiat 500	30.5	36.5
Fiat Panda	31.5	37.5
Fiat Tipo	31	40.5
Fiat Doblo	31	40.5
Fiat Fiorino	32	37
Fiat Linea	28.5	35
Fiat 500X	30	46
Fiat 500L	31.5	38.5
Alfa 159	28	34
Honda Civic	27	32.5
Opel Corsa	28.5	31.5
Opel Zafira	30	42
Škoda Octavia II.	32	40.5
Škoda Fabia	29.8	38
Škoda Yeti	29	38.5
Kia Sportage	37.5	47.5
Peugeot 207	27.5	36
Average	30.31	38.35
Minimum Distance	27	31.5
Maximum Distance	37.5	47.5

The values were obtained by direct manual measurements with measuring tape of representative passenger vehicles.

Based on the results of measurements, it was defined that the maximum distance of lifting should be 47.5 cm.

2.2. Maximum Load Capacity

Another important aspect regarding the requirements is the maximum permissible weight that the device can lift. This weight defines the load capacity of the aid, which must be ensured throughout the entire range of movement.

In the case of an aid for boarding a vehicle, the load capacity refers to the weight of a person's legs. This weight is determined by calculating the mass of the relevant body part. The weight of individual parts of the human body can be established using two approaches, both of which are based on the total body weight. The first approach utilizes a method in which the total body weight is distributed as percentages to individual body parts. This method is greatly inaccurate, as it does not consider the overall height. A relatively precise method used for such calculations is known as the Zatsiorsky method, which considers the total height of the individual. Its accuracy is based on research conducted on 100 subjects

using the radioisotope method, which measures the attenuation of radiation as it passes through different segments of the body. After processing the research data using regression equations, coefficients were determined for calculating the mass of each body part [25].

The weight of individual body parts is calculated using coefficients according to the following formula:

$$m_i = B_0 + B_1 \times x_1 + B_2 \times x_2 \quad (1)$$

m_i—weight of the i-th segment (kg);
B_0, B_1, B_2—coefficients;
x_1—total body weight of the person (kg);
x_2—total body height of the person (cm).

For the calculation, we used average values of the total body weight and total body height as determined from the CATIA V5 database. To achieve the broadest possible coverage of the European population, we utilized values available for both the German and French nationalities, within the range of the 1.9th to 100th percentile. The average height, leg length, and body weight of the German and French populations are given in Tables 2 and 3.

Table 2. Average height, leg length, and body weight of the German population.

German Population			
Percentile	1.9	50	100
	Body Height (mm)		
Male	1612.9	1750	2014
Female	1508.4	1625	1849.8
	Leg Length (mm)		
Male	727.1	813.2	979.2
Female	698.4	766.2	896.8
	Body Weight (kg)		
Male	66.1	79	122.9
Female	53.6	66	95.4

Table 3. Average height, leg length, and body weight of the French population.

French Population			
Percentile	1.9	50	100
	Body Height (mm)		
Male	1612.2	1744.8	2000.4
Female	1493.9	1621.2	1866.4
	Leg Length (mm)		
Male	756.6	846.9	903.5
Female	687.5	769.4	819.9
	Body Weight (kg)		
Male	34.1	70.6	109.6
Female	28.6	58.4	77.7

Based on the values above, Table 4 was constructed.

Table 4. Average height, average weight, maximum average height and maximum average Weight in our case.

	Average Height (mm)	Average Weight (kg)	Maximum Average Height (mm)	Maximum Average Weight (kg)
Male	1747.4	74.82	2007.2	116.25
Female	1623.1	62.2	1857.9	86.55

When substituting the obtained average values into the formula for calculating the weights of body segments, the resulting weight represents the load that the device must support during its operation. For the calculation, we used both the average values and the maximum average values for males to account for the maximum possible usage of the device. Average values for the weights of individual body parts are given in Tables 5 and 6.

Table 5. Weight of individual body parts—Average value [26].

Segment	%	B_0 [kg]	B_1	B_0 [kg/cm]	Zatsiorski Method
Head	7.4%	1.296	0.0171	0.0143	5.074204
Thigh	12.40%	−2.649	0.1463	0.0137	10.691104
Knee	4.60%	−1.592	0.03616	0.0121	3.2278452
Foot	1.6%	−0.829	0.0077	0.0073	1.022716
Upper Arm	2.90%	0.25	0.03012	−0.0027	2.0317804
Forearm	1.7%	0.3185	0.01445	−0.00114	1.2004454
Hand	0.70%	−0.1165	0.0036	0.00175	0.458647
Torso	44.80%				32.6112964
Upper Part of Torso		8.2144	0.1862	−0.0584	11.941068
Middle Part of Torso		7.181	0.2234	−0.0663	12.310526
Lower Part of Torso		−7.498	0.0976	0.04896	8.3597024
Upper Limb, Total					3.6908728
Lower Limb, Total					14.9416652
Total					**74.9505764**

Table 6. Weight of individual body parts—Maximum average value [26].

Segment	%	B_0 [kg]	B_1	B_0 [kg/cm]	Zatsiorski Method
Head	7.4%	1.296	0.0171	0.0143	6.153885
Thigh	12.40%	−2.649	0.1463	0.0137	17.107965
Knee	4.60%	−1.592	0.03616	0.0121	5.04007
Foot	1.6%	−0.829	0.0077	0.0073	1.531235
Upper Arm	2.90%	0.25	0.03012	−0.0027	3.20956
Forearm	1.7%	0.3185	0.01445	−0.00114	1.7695145
Hand	0.70%	−0.1165	0.0036	0.00175	0.653225
Torso	44.80%				51.658382
Upper Part of Torso		8.2144	0.1862	−0.0584	18.13927
Middle Part of Torso		7.181	0.2234	−0.0663	19.84484
Lower Part of Torso		−7.498	0.0976	0.04896	13.674272
Upper Limb, Total					5.632995
Lower Limb, Total					23.67927
Total					**116.435406**

The Zatsiorski method is used to estimate body-segment masses from body height and body weight, and this will be stated unambiguously.

Based on the calculated values, the weight of one leg at the average value is 14.94 kg, and at the maximum average value is 23.7 kg. Consequently, the average load on the device will be 29.88 kg, and the maximum load will reach 47.4 kg. For safety reasons, we adjusted the calculated values by a safety factor of 20%, represented by a safety coefficient of k = 1.2. Such a coefficient was chosen to keep the device lightweight. Accordingly, the average and maximum average loads on the device, when considering the safety factor, increase from 29.88 kg to 35.86 kg and from 47.4 kg to 56.88 kg, respectively.

2.3. Leg Lifter Mechanism Choice

Several principles can be used to lift an object up. We considered the following principles:

- Hydraulic—powerful with a relatively small size, but in case of failure, it goes down without the possibility to stop it. It can injure the person whose legs are placed on the lifter. To avoid this, it is necessary to use a mechanical security system (ratchet mechanism), which makes construction more complicated and heavier.
- Pneumatic—pneumatic drive offers fast lifting in comparison with hydraulic, but it is noisy and needs a source of compressed air. Another possibility is using pneumatic balloons, like those in pneumatic balloons jacks. This is a simple solution, and with a safety valve, it is safe for use, but usually not very precise.
- Mechanics—there can be many different solutions, e.g.,
    a. Linear drive unit—safety, precise but expensive solution.
    b. Lever mechanism—in this case, not very suitable, because of the small space and relatively high distance of lifting.
    c. Pulley mechanism—simple, reliable, and precise but more suitable to lift in one point. To lift a surface on a horizontal plane, it will require more pulleys or an equal distribution of force to at least three points. It can require a more complex mechanism to facilitate equal lifting at all points of anchorage. Moreover, there can be problems with ropes, which can tangle.
    d. Screw mechanism—e.g., scissor lift. Robust, inexpensive, precise and simple.

After considering the following criteria: lifting height, stability, self-locking, portability, simplicity and manufacturability, a scissor lift with a screw mechanism was chosen. A sketch of the initial design is shown in Figure 1.

Figure 1. Leg lifter sketch.

3. Results

In designing the aid, there was effort to minimize the height of the device while ensuring the maximum possible lifting height, considering the construction and dimensions of the aid. For devices that are not an integral part of the vehicle, it is particularly important to achieve the lowest possible weight and to ensure the ease of handling.

The structure rests on the ground through the bottom frame and is intended to be equipped with anti-slip rubber contact elements on the underside of the base. These increase friction against the pavement and prevent uncontrolled sliding during boarding.

As part of the solution, we developed a design for an aid to facilitate boarding and alighting from vehicles for individuals with reduced mobility, with an emphasis on achieving the simplest possible construction and the greatest possible universality of use, which is ensured by a wide range of applicability across various types of vehicles. The design

focuses on minimizing the height of the device, ease of use, and simplicity of construction, which collectively result in the lowest possible cost. In this proposal, the device is positioned by an accompanying person near the vehicle, while the operation itself is performed by the individual with limited mobility.

The structure consists of a primary frame, referred to as the base, which houses all the moving parts responsible for lifting the platform. The lifting mechanism is facilitated by arms anchored to the base or the platform on one side, while the other end of the arms moves within guiding grooves, assisted by a bearing located at the end of a shaft. The stability of the entire structure depends significantly on the rigidity of both the base and the platform. Stability and rigidity are further enhanced using axial bearings in the mutually rotating components. The use of such bearings also reduces friction throughout the assembly.

The upper platform, which serves as the support surface for the feet during lifting, is composed of several parts. The top part features a non-slip surface to secure the position of the feet on the platform, while the lower part ensures the rotary mounting of the arms and their guidance along the designated tracks. The space between the upper and lower parts of the platform is used to accommodate an extension plate, which fills the gap between the vehicle and the leg lifter, thus allowing for the easy transfer of the legs from the device into the vehicle.

When actuating the aid, a power screw and nut assembly in various configurations may be used, each offering distinct advantages and disadvantages. When using a power screw drive, rotational motion (torque) is converted into linear motion (axial force). It is also possible to convert linear motion into rotary motion, but only if screws with a thread angle greater than the friction angle are used, i.e., screws that do not meet the condition of self-locking.

3.1. Main Components of the Power Screw

The main components of the power screw are the following:

- Power screw with a specific thread type;
- Nut;
- Source of rotational motion.

In the proposed design, the driving component is an electric motor that drives the power screw, which is rotatably mounted in the base of the device. Through the rotational movement of the screw, the movable nut provides linear actuation. The movable nut is equipped with two pins to which the lifting arms are attached. These arms are terminated with bearings that serve as guides for the nut within the base [27].

Evaluation of the Proposed Design

The proposed solution possesses both advantages and disadvantages that determine its suitability for assisting individuals with partial mobility impairments in boarding vehicles. Some of the disadvantages can be addressed through modifications to the design or by utilizing various types of actuators, each of which offers specific properties; in some cases, a combination of multiple actuators can achieve the desired characteristics.

The advantages are as follows:

- Simple, stable construction composed of standardized components;
- Straightforward and cost-effective drive mechanism;
- Low weight;
- Design independent of the vehicle;
- High universality.

The disadvantages are as follows:

- Requirement for a compact, high-performance motor, a drawback that can be mitigated by employing linear actuators;
- Reduced stability on uneven terrain.

In the design process, there was an effort to achieve maximum universality and simplicity of construction, resulting in ease of manufacturing and a low cost. Alongside these features, the device must maintain the lowest possible height while providing the highest possible lifting range. As was mentioned, the leg lifter is designed such way that it is not integrated with the vehicle, given the requirements for homologation and the potential impact on the vehicle's structural components.

A detailed design process is preceded by the determination of requirements that the device must fulfil. By meeting the specified requirements, the correct functioning of the device is ensured.

3.2. Model Creation

For the creation of the virtual model, the SolidWorks 2017 software was chosen. To create a CAD model, solid modeling techniques were used. The modeling was based on the initial design of the aid, where a simple scissor mechanism was employed that, through its construction and dimensions, meets the requirements for lifting heights. If it becomes necessary to use the device for light commercial and delivery vehicles, the structure can be supplemented with an additional pair of arms, thereby increasing the lifting height. However, the addition of another pair of arms would reduce the stability of the platform. The base of the device was constructed using U-profiles connected by a flat bar. The platform guidance was realized by ball bearings traveling within the U-shaped guide profiles. In constructing the virtual model, standardized components and semi-finished products were used to simplify manufacturing and minimize the need for custom-made parts.

The base frame was designed from a U-profile of 30 × 10 × 10 × 2 mm. In the numerical model, the material was aluminum, while for the prototype, steel was used due to the manufacturing cost and availability.

The U-profile 30 × 10 × 10 × 2 mm used in the base frame has a cross-sectional area of 92 mm^2, second moment of area about the strong axis $I_x = 1.078 \times 10^4$ mm^4, and section modulus $W_x = 7.19 \times 10^2$ mm^3. Under the design load of 588.6 N, assuming symmetrical load transfer, one side profile carries 294.3 N. For a conservative beam-based estimate over the characteristic length 251 mm, the maximum bending moment is 18.47 Nm and the resulting bending stress is 25.7 MPa, confirming sufficient stiffness and strength of the selected section.

Assembly of the device is shown in Figure 2.

A local check of the weakened U-profile cross-section in the bolted/pinned connection zone was added. Using the internal force $F_1 = 3295.98$ N and a conservative hole diameter of 10 mm, the net area of the two profile walls is 80 mm^2, which gives a net-section stress of 41.2 MPa. The result confirms that the profile remains safely within the allowable stress range in the connection zone.

To ensure that the device will work, safety calculations were carried out. The main mechanical principle used in the device is a power screw mechanism. There are many sources that address power screw calculation [28–35]. For theoretical information research and integration of the knowledge gained, the following calculations were carried out.

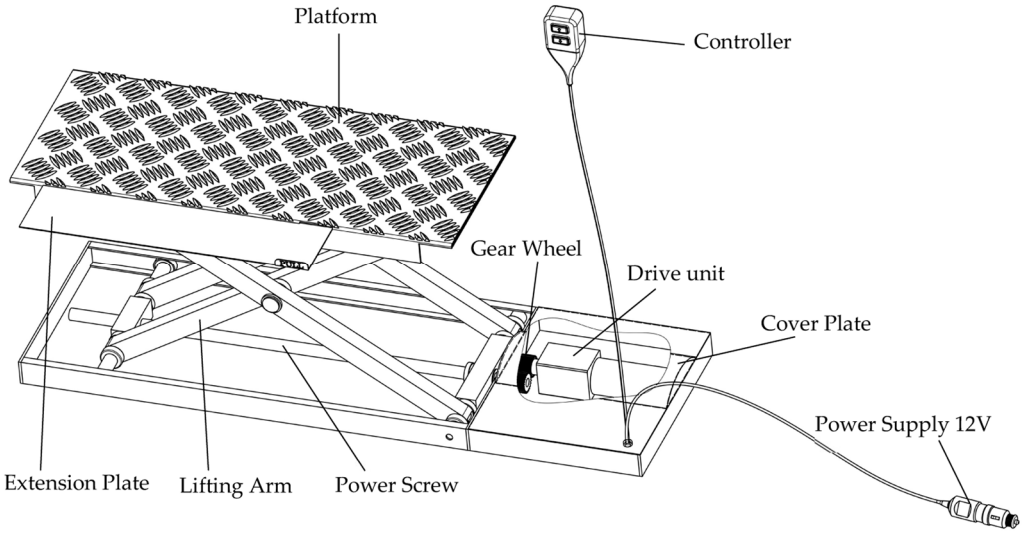

Figure 2. Leg lifter sketch.

3.3. Calculations

3.3.1. Calculation of the Power Screw

Axial Force

The device is subjected to a gravitational force F, which consists of the weight of the user's legs with limited mobility resting on the platform and the weight of the platform itself. Together, they total 60 kg, i.e., 588,6 N. Based on the applied force F, we calculated the axial force acting within the assembly screw, which is necessary for its strength verification.

The local wall bearing stress in the U-profile at the bolt/pin hole was also evaluated. For the critical internal force 3295.98 N, profile thickness 2 mm, and hole diameter 10 mm, the calculated bearing pressure is 82.4 MPa. This value is acceptable for the steel prototype; therefore, no significant ovalization of the hole is expected under the considered static loading.

Transformation of the Assembly into a Planar System of Bodies

Assembly was transformed into a planar system of bodies, consisting of two bodies represented by rods, which are interconnected by a joint. The individual reactions at the connections are defined by forces.

The loading force is at the edge (e.g., in Figures 3, 5 and 7–9) because this represents the largest load case, and if the structure can withstand this load, it can also withstand the normal load, where the force is at the center of the platform.

The planar system of bodies is shown in Figure 3.

Release of system members

First Body in the Plane
A—pivot point;
$\beta = 5^{\circ}$;
$l_1 = 224$ mm;
$l_2 = 251$ mm;
A_x, A_y, F_1, N_2—unknown forces.
Release of the first body in the plane is shown in Figure 4.

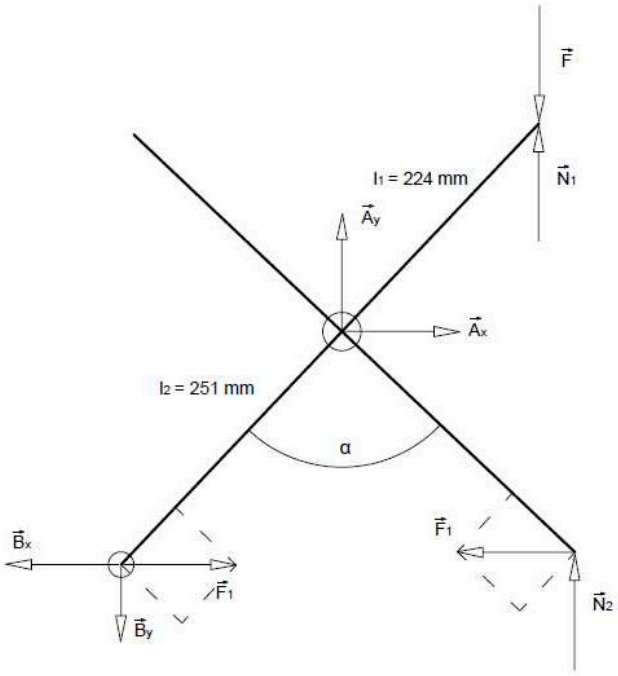

Figure 3. Planar system of bodies.

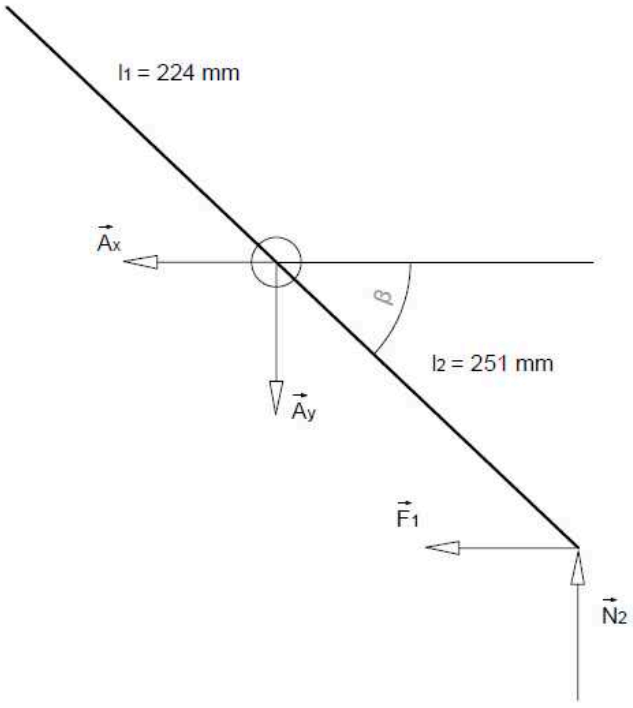

Figure 4. Releasing the first body in the plane.

Conditions of Static Equilibrium:

$$\sum F_{ix} = 0; -Ax - F_1 = 0 \quad (2)$$

$$\sum F_{iy} = 0; -Ay + N_2 = 0 \quad (3)$$

$$\sum (Mi)A = 0; -F_1 \times l_2 \times \sin\beta + N_2 \times l_2 \times \cos\beta = 0 \quad (4)$$

Second Body in the Plane

A—pivot point;

β = 5°;
F = 588.6 N;
l_1 = 224 mm;
l_2 = 251 mm;
A_x, A_y, B_x, B_y, F_1—unknown forces.
Release of the second body in the plane is shown in Figure 5.

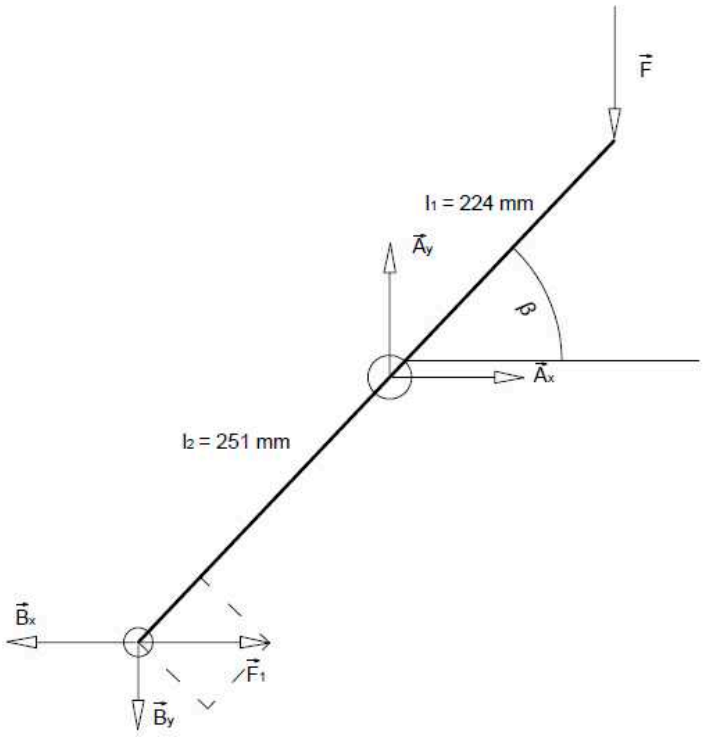

Figure 5. Releasing the second body in the plane.

Conditions of Static Equilibrium:

$$\sum Fix = 0;\ Ax + F_1 - Bx = 0 \quad (5)$$

$$\sum Fiy = 0;\ -F + Ay - By = 0 \quad (6)$$

$$\sum (Mi)A = 0;\ -F \times l_1 \times \cos\beta + F_1 \times l_2 \times \sin\beta + By \times l_2 \times \cos\beta - Bx \times l_2 \times \sin\beta = 0 \quad (7)$$

System of Equations

$$-Ax - F_1 = 0 \quad (8)$$

$$-Ay + N_2 = 0 \quad (9)$$

$$-F_1 \times l_2 \times \sin\beta + N_2 \times l_2 \times \cos\beta = 0 \quad (10)$$

$$Ax + F_1 - Bx = 0 \quad (11)$$

$$-F + Ay - By = 0 \quad (12)$$

$$-F \times l_1 \times \cos\beta + F_1 \times l_2 \times \sin\beta + By \times l_2 \times \cos\beta - Bx \times l_2 \times \sin\beta = 0 \quad (13)$$

After Adjustment:

$$-Ax - F_1 = 0 \quad (14)$$

$$-Ay + N_2 = 0 \quad (15)$$

$$-F_1 \times l_2 \times \sin\beta + N_2 \times l_2 \times \cos\beta = 0 \quad (16)$$

$$Ax + F_1 - Bx = 0 \quad (17)$$

$$Ay - By = F \quad (18)$$

$$F_1 \times l_2 \times \sin\beta + By \times l_2 \times \cos\beta - Bx \times l_2 \times \sin\beta = F \times l_1 \times \cos\beta \quad (19)$$

Augmented Matrix of the System:

$$\begin{pmatrix} -1 & -1 & 0 & 0 & 0 & 0 & 0 \\ 0 & 0 & -1 & 0 & 0 & 1 & 0 \\ -\frac{547}{25} & 0 & 0 & 0 & 0 & \frac{547}{25} & 0 \\ 1 & 1 & 0 & -1 & 0 & 0 & 0 \\ 0 & 0 & 1 & 0 & -1 & 0 & 589 \\ \frac{547}{25} & 0 & 0 & -\frac{547}{25} & \frac{547}{25} & 0 & \frac{656,723}{5} \end{pmatrix}$$

The system matrix was transformed into triangular form using the Gaussian elimination method.

$$\begin{pmatrix} -1 & -1 & 0 & 0 & 0 & 0 & 0 \\ 0 & \frac{547}{25} & 0 & 0 & 0 & \frac{547}{25} & 0 \\ 0 & 0 & -1 & 0 & 0 & 1 & 0 \\ 0 & 0 & 0 & -1 & 0 & 0 & 0 \\ 0 & 0 & 0 & 0 & -1 & 1 & 589 \\ 0 & 0 & 0 & 0 & 0 & \frac{1094}{25} & 144,232 \end{pmatrix}$$

The matrix in triangular form was rewritten as a system of equations:

$-F_1 - Ax = 0 \Rightarrow F_1 = 3295.98$ N
$\frac{547}{25} \times Ax + \frac{547}{25} \times N_2 = 0 \Rightarrow Ax = -3295.98$ N
$-Ay + N_2 = 0 \Rightarrow Ay = 3295.98$ N
$-Bx = 0 \Rightarrow Bx = 0$
$-By + N_2 = 589 \Rightarrow By = 2706.98$ N
$\frac{1094}{25} \times N_2 = 144.232 \Rightarrow N_2 = 3295.98$ N

By substituting the values into the system of equations derived from the matrix in triangular form, we calculated the required axial force in the screw as $F_1 = 3295.98$ N.

Strength Verification of the Power Screw

Power screws are subjected to various types of stresses during operation, namely torsion, tension, and compression. In cases where the length of the screw is significantly greater than its diameter, buckling must also be considered. Screw M12×1.75 is considered for leg lifter.

Tensile/Compressive Stress in the Core of the Screw (σ):

$$\sigma = \frac{4 \times F_Q}{\pi \times d_3^2} = \frac{4 \times 3295.98\ \text{N}}{\pi \times 9.853^2\ \text{mm}} = 43.22\ \text{MPa} \quad (20)$$

F_Q—Axial Force in the Screw;
d_3—Minor Diameter of the External Thread at the Crest of the Thread Root Radius.
Shear Stress in Torsion (τ_k):

$$\tau_k = \frac{Mtz}{Wk} = \frac{0.5 \times F_Q \times d_2 \times \text{tg}(\gamma + \varphi)}{\frac{\pi \times d_3^3}{16}} = \frac{0.5 \times 3295.98\ \text{N} \times 10.863\ \text{mm} \times tg(2.94^\circ + 6.84^\circ)}{\frac{\pi \times 9.853^3 \text{mm}}{16}} = 16.43\ \text{MPa} \quad (21)$$

M_{tz}—Frictional Torque in the Thread of the Screw and Nut;
W_k—Torsional Section Modulus.
d_2—Pitch Diameter.

γ—Lead Angle of Thread (M12×1.75).
φ—Friction Angle for Friction Coefficient μ=0.12.
Reduced Stress:

$$6_{red} = \sqrt{6^2 + 3\tau_k^2} \leq 6dov = \sqrt{43.22^2\ \text{MPa} + 3 \times 16.43^2\ \text{MPa}} = 51.75\ \text{MPa} \quad (22)$$

$$6_{dov} = \frac{6_{kt}}{k} = \frac{265}{4} = 66.25\ \text{MPa} \quad (23)$$

k—Safety Factor (1 ÷ 5);
6_{kt}—Yield Strength (steel grade E295–265 MPa).

$$6_{dovred} = \frac{6_{dov}}{\beta_{pr}} = \frac{66.25\ \text{MPa}}{1.2} = 55.2\ \text{MPa} \quad (24)$$

β_{pr}—determined by estimation ≈ 1.2.
Minimum Minor Diameter of the External Thread d_3:

$$d_3 \geq 2 \times \sqrt{(F_Q/(\pi \times 6\_dovred))} = \sqrt{(3295.98\ \text{N}/(\pi \times 55.2\ \text{MPa}))} = 8.72\ \text{mm} \quad (25)$$

$d_3 \geq 8.72$ mm.
Verification of the Accuracy of the Estimated Coefficient β:

$$\beta = \sqrt{1 + 3 \times \left[\frac{d+d_3}{d_3} \times tg(\gamma + \varphi)\right]^2} = \sqrt{1 + 3 \times \left[\frac{12\ \text{mm}+9.853\ \text{mm}}{9.853\ \text{mm}} \times tg\ (2.94^\circ + 6.84^\circ)\right]^2} = 1.199$$
$$\beta = 1.2 \leq \beta pr \quad (26)$$

d—Major Diameter.
Verification of the Specific Pressure in the Threads p:
$p = \frac{F_0}{\pi \times d_2 \times v_z \times z} \leq p_{dov} = \frac{3295.98\ N}{\pi \times 10.863\ \text{mm} \times 1.0735 \times 14.28} = 6.3$ MPa
$p = 6.3\ \text{MPa} \leq p_{dov}$.

$$v_z = \frac{(d - d_3)}{2} = \frac{(12\ \text{mm} - 9.853\ \text{mm})}{2} = 1.0735\ \text{mm} \quad (27)$$

v_z—Thread Engagement Depth;
z—Number of Threads in the Nut;
p_{dov}—Permissible Specific Pressure (15 ÷ 20 MPa).

3.3.2. Calculation of Drive System

To drive the power screw, it is proposed an electric motor with a gearbox, which were selected based on measurements performed on the physical model. Measured values of torque are given in Table 7.

These measurements were used to determine the torque required for selecting a suitable electric motor and gearbox for the physical implementation of the concept. To measure torque, a force gauge was used. The force gauge was attached to a lever with length 0.25 m. One end of the lever was attached to a power screw. Then, a load was placed on the leg lifter. By pulling the force gauge placed on the opposite side of the lever, the power screw was rotated to move the load up, and the force was measured. When the weight is 0 kg, 0.28 Nm torque is necessary to lift the platform of the device because of the weight the platform itself and friction in the tread of the power screw.

Table 7. Measured values of torque.

Weight (kg)	1. Measurement (N)	2. Measurement (N)	Average (N)	Torque (Nm)
0	1.04	1.2	1.12	0.28
10	5.2	4.2	4.7	1.175
20	7.5	7.5	7.5	1.875
30	10	11.1	10.55	2.6375
40	13.5	11.44	12.47	3.1175
50	14.6	13.6	14.1	3.525
60	22.3	18	20.15	5.0375
70	22	20	21	5.25
80	22	23.7	22.85	5.7125

Based on the measured values, it follows that an electric motor with a torque of approximately 5.04 Nm is required to drive the device. This value results from the basic load capacity requirement of 56.88 kg, which is approximately equivalent to the measurement with a 60 kg weight (including platform weight).

Gearbox

For the gearbox, the key parameters are the output speed and the input speed necessary to achieve it. Based on the required lifting height, we calculated the necessary rotational speed as follows:

Average lifting height: 383.5 mm

- To lift the platform to a height of 383.5 mm, the nut must travel 159 mm.
- The pitch of the screw is 1.75 mm.

$$\text{Rotational Speed} = \frac{\textit{Required distance}}{\textit{Thread Lead}} = \frac{159\ \text{mm}}{1.75\ \text{mm}} = 91\ \text{revolutions} \quad (28)$$

- The lead screw must complete 91 revolutions to achieve a lifting height of 383.5 mm.
- The time required for the lift was empirically determined to be 30 s.

$$\text{Motor Speed} = \frac{1 \textit{minute} \times \textit{required revolutions}}{\textit{Lifting Time}} = \frac{1 \times 91}{0.5} = 182\ \text{rpm} \quad (29)$$

- The calculation shows that, for the average lifting height, a rotational speed of 182 rpm is required to raise the platform within the specified time of 30 s.

Maximum Lifting Height: 475 mm

- To lift the platform to a height of 475 mm, the nut must travel 308 mm.
- The pitch of the screw is 1.75 mm.

$$\text{Revolutions} = \frac{\textit{Required Distance}}{\textit{Thread Lead}} = \frac{308\ \text{mm}}{1.75\ \text{mm}} = 176\ \text{revolutions} \quad (30)$$

- The lead screw must complete 176 revolutions to achieve a lifting height of 475 mm.
- The time required for the lift was empirically determined to be 30 s.

$$\text{Motor Speed} = \frac{1 \textit{minute} \times \textit{required revolutions}}{\textit{Lifting Time}} = \frac{1 \times 176}{0.5} = 352\ \text{rpm} \quad (31)$$

- The calculation shows that, for the maximum lifting height, a rotational speed of 352 rpm is required to raise the platform within the specified time of 30 s.

Based on the calculated values, we selected the CGI 017VPX gearbox with a gear ratio of 15:1. Parameters of the gearbox are given in Tables 8 and 9.

Table 8. Gearbox parameters.

CGI 017VPX (CN)			
Ratio	**M_{nom} (Nominal) (Nm)**	**M_{start} (Starting) (Nm)**	**M_{max} (Maximal) (Nm)**
4:1	12	16	25
5:1	12	15	24
7:1	10	13	21
10:1	9	12	17
15:1	12	16	25
20:1	14	17	28
25:1	13	16	26
28:1	14	17	28
40:1	14	18	29
50:1	13	17	27
70:1	11	14	23
100:1	9	12	17

Table 9. Additional gearbox data.

Gearbox Weight	**Single-Stage 0.36 kg/Two-Stage 0.5 kg**
Input Speed	Maximal 5000 rpm
Gearbox Backlash	0.2° (Single-stage), 0.26° (Two-stage)
Degree of Protection—IP	IP54
Service Life	>10,000 h
Efficiency	Single-stage > 90%/Two-stage > 85%
Operating Temperature	−40 °C to 120 °C

Electric motor

For the selected gearbox, we chose a motor that meets the gearbox's input parameters, such as a maximum speed of 5000 rpm. We also chose the Jkong 42ZTY04B motor. The parameters are presented in Table 10.

Table 10. Electric motor parameters.

Model	**42ZYT04B (CN)**	
	Unit	**Value**
Rated Voltage	V	12
Continuous Rated Speed	rpm	4700
Continuous Rated Torque	mN.m	100
Direct Current	A	5.85
Starting Torque	mN.m	479
Starting Current	A	26.71
No-load Speed	pm	5900
No-load Current	A	0.4
Demagnetization Current	A	52
Rotor Inertia	g/cm^2	154
Motor Weight	g	550
Motor Length	mm	90

The electric motor with a gearbox is connected to the lead screw by means of spur gears, as the gearbox output shaft is offset from the axis of the lead screw. This misalignment of axes is caused by the location of the gearbox output shaft and the dimensions of the gearbox.

If a custom-built electric motor with a gearbox is used, direct coupling may be employed, with the gearbox output speed and motor speed corresponding to the calculated values.

Control and Power Supply

The device is powered by the vehicle's 12 V electrical system, to which it is connected via a car lighter socket connector or, alternatively, a 12 V automotive power outlet. Additional installation of an external automotive socket near the door, or the use of an extension socket, is possible to facilitate easy connection of the device.

Control of the device is provided by a simple controller with a pair of non-latching switches. A useful feature is the ability to regulate the motor speed directly on the controller, allowing adjustment of the lifting speed. To eliminate the need for electrical wiring, a wireless controller may also be used. Figure 6 shows the complete CAD model of the proposed device.

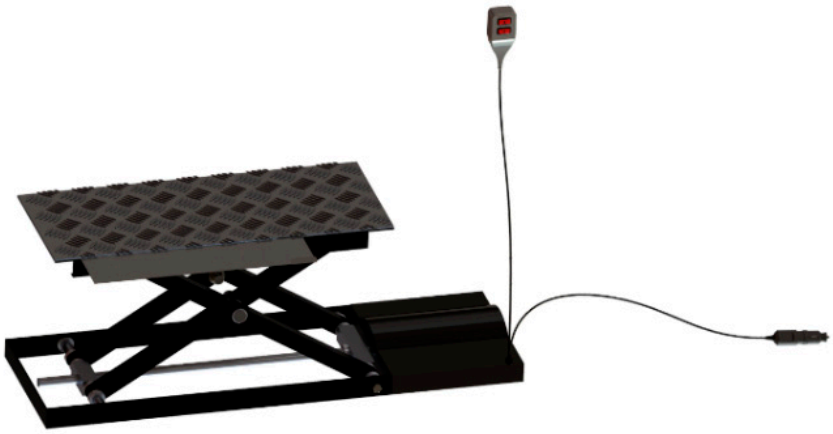

Figure 6. Complete CAD model of the proposed device.

3.3.3. Static Analysis

After producing the detailed CAD model of the device (Figure 6), a static analysis was conducted to verify the overall rigidity of the proposed structure. The assembly was subjected to static analysis. As a first step, an idealized assembly was created by removing all parts and fillets that do not affect the simulation results. This idealization simplified and accelerated the meshing of the assembly, as well as the final computation, in which we evaluated stresses within the structure, as well as deformations and displacements resulting from the applied forces. In the simulations, a loading force of F = 588.6 N was set, which corresponds to the maximum calculated load from the user's legs, along with the weight of the assembly itself. During the simulations, the assembly was subjected to critical loading conditions representing the worst-case scenario. Under this critical load, the force acts at the edge of the lifting platform in the area guiding the lifting arms.

Figure 7 displays stress in the assembly, represented by a color gradient ranging from blue to red, where blue indicates minimum (zero) stress and red indicates maximum stress in the assembly. The maximum stress in the assembly is 94.091 MPa, which occurs at the movable nut in connection with the radial bearing.

The displacement in the assembly is represented by the same color scale as the stress distribution in Figure 8. For visualization, a deformation display was used, which presents the model in its deformed state at the corresponding scale. The maximum displacement in the assembly is defined at the point of application of the loading force, with a value of 1.734 mm.

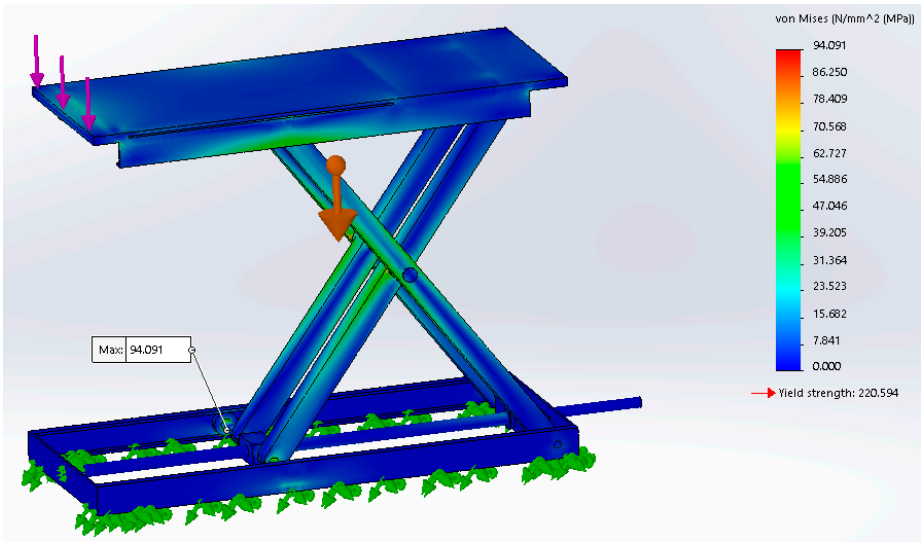

Figure 7. Stress in the assembly. Purple arrows represent external load, green arrows represent fixed geometry and big arrow in middle showing gravity.

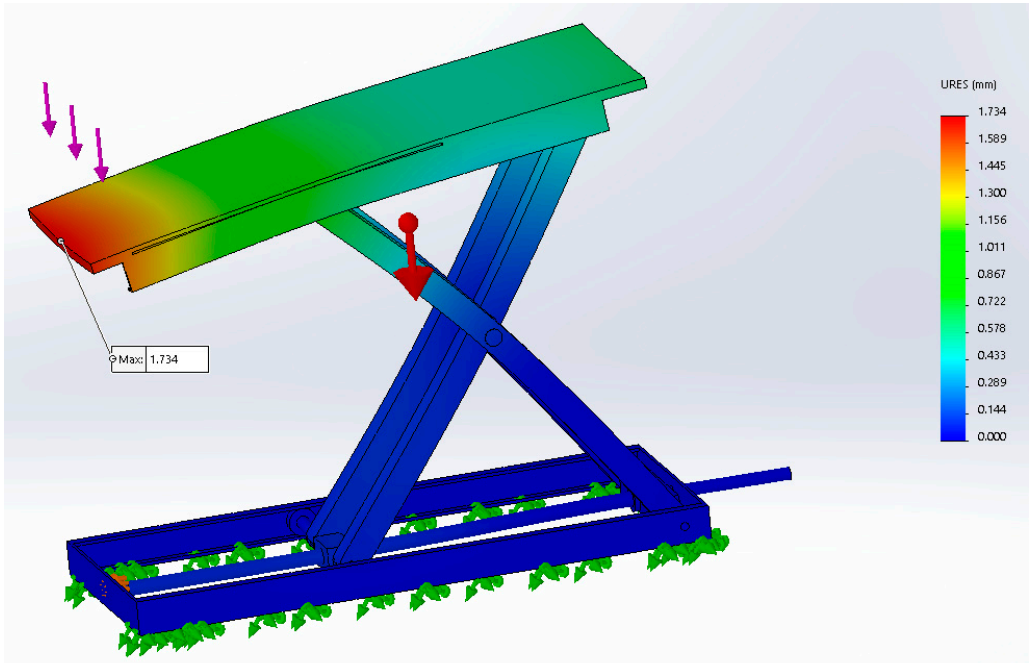

Figure 8. Deformation displacement visualization in the assembly. Purple arrows represent external load, green arrows represent fixed geometry and big arrow in middle showing gravity.

Relative deformation (Figure 9) uses color to depict the change in length caused by the applied forces relative to the original length. The highest relative deformation is observed at the connection point between the movable nut and the radial bearing.

Simulation results indicate that the structural design of the device is sufficient with respect to the applied forces. According to the measured values, the structure is over-dimensioned. This over-dimensioning allows for further modifications to the design, such as reducing the overall weight of the device.

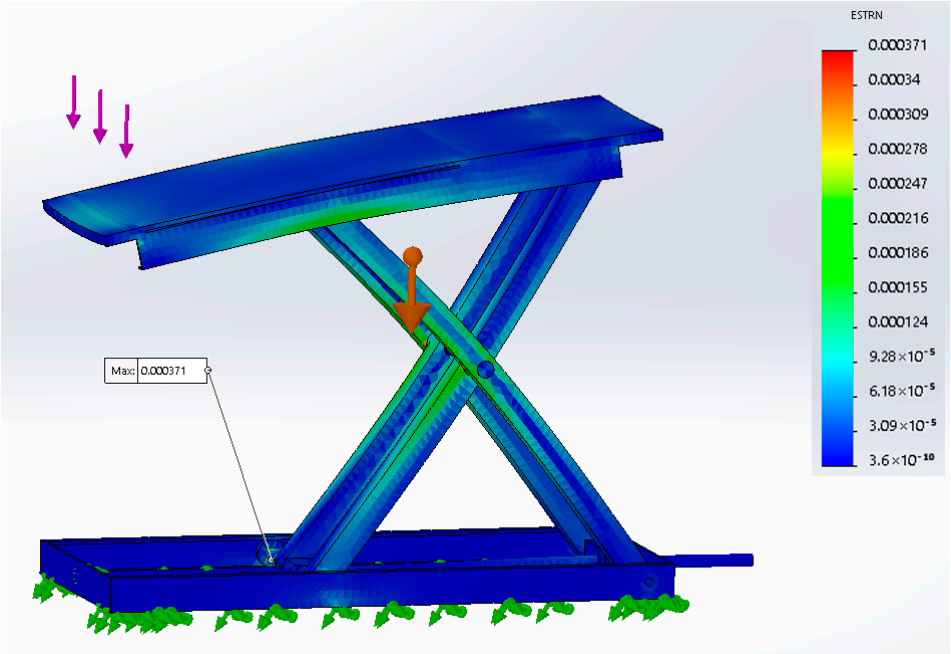

Figure 9. Visualization of relative deformation. Purple arrows represent external load, green arrows represent fixed geometry and big arrow in middle showing gravity.

4. Discussion

After designing the structure of the device and verifying its correctness through calculations and simulations, the prototype was produced. Due to cost considerations, steel was used instead of the originally proposed aluminum material.

The production process of the device is given in Figure 10.

Figure 10. Production process of the leg lifter.

During prototype production, we utilized milling, turning, and bending technologies. The individual parts were assembled using bolting, MIG welding, and riveting. The fabrication of each component was preceded by the preparation of technical drawings based on the CAD model. To the greatest extent possible, we sought to use standardized products and semi-finished materials, thereby reducing the need for machining and lowering the cost of the device. At the final stage of production, layers of two-component primer and protective topcoat were applied to the completed structure. The completed device is shown in Figure 11.

Usage of device

1. Open the vehicle door and place the device parallel to the wheel well of the vehicle.
2. Stand on the device with your back to the vehicle and then sit down on the seat. It is advisable to use a swivel seat cushion placed on the seat.
3. Lift the legs of the person with partial mobility impairment to the required height.
4. Transfer the legs into the vehicle using the sliding element.
5. Fold and store the device.

Figure 11. Completed device.

The present paper is focused on the engineering design, analytical assessment, structural verification, and prototype realization of the device. It was not intended as a full experimental-validation study; therefore, user evaluation, fatigue testing, and repeated-cycle durability assessment were not included within the scope of this work. In this sense, the manuscript addresses the feasibility and structural functionality of the concept rather than its long-term operational validation.

The sequence of leg lifter use is shown in Figure 12.

Figure 12. Sequence of leg lifter use.

The proposed leg lifter is a result of original research, development, and production under universities in the Slovak Republic. The contribution of the paper is a vehicle-independent powered transfer platform for assisted boarding, designed to support both

lower limbs continuously during transfer and allow controlled powered repositioning with intermediate stopping, as structurally validated by anthropometric load estimation, analytical calculations, and finite-element analysis.

5. Conclusions

Demographic developments in society predict a significant increase in the number of people in older age categories. As the population ages, morbidity also rises, resulting in decreased mobility. Consequently, there is an increasing need to address mobility challenges through the development of assistive devices and equipment.

This paper is therefore devoted to addressing the issue of mobility by means of a device designed to facilitate boarding and alighting from vehicles. After market research, we a identified market gap—there is no such device with the required parameters.

This paper focuses on the potential to eliminate that shortcoming through the design of a device with a high degree of universality. That design was elaborated on in detail. The universality and correct functionality of the design were ensured through measurements and calculations, which represent the basic input data for determining the parameters of the device. After processing the input data, a model of the proposed device was created in SolidWorks using volume modeling. This model allowed the design to be tested in a virtual environment and served as the basis for strength analyses. Before performing the strength analyses, an idealized model was created, derived from the virtual model and simplified to the greatest possible extent. Strength analyses were carried out in the SolidWorks Simulation module, focusing on verifying the rigidity of the structure. The results are presented as visualizations of stress and deformation within the assembly, enabling the identification of critical areas in the design. After the strength analyses, the design exhibited high structural rigidity, indicating an over-dimensioned structure, which can be optimized and lightened through appropriate modifications. The advantages of the proposed device lie mainly in its simplicity and universality, making it suitable for various types of automobiles. The principal contribution of this solution is the facilitation of boarding and alighting for people with partial mobility impairments.

After evaluating and verifying the correctness of the design, the prototype was made, utilizing machining, cutting, and joining technologies. The prototype was produced based on technical drawings derived from the virtual model of the device, with the production of individual components and subsequent assembly—including surface finishing. Based on the prototype testing, there were some problems that require improvements to the design, which will be the subject of future work.

The novelty of this work is not the control strategy or mathematical optimization. Instead, it lies in the mechanical and functional concept of a universal powered lower-limb transfer platform intended for assisted vehicle boarding, including continuous support of both legs, controlled lifting, intermediate-position stopping, and usability across different vehicle types without permanent vehicle modification. In our view, this represents the main advancement over common passive leg-lifting aids and defines the contribution of the current paper.

Author Contributions: Conceptualization, A.M. and T.M.; methodology, P.M.; software, A.M.; validation, Z.Š. and N.D.; formal analysis, N.D.; investigation, P.M.; resources, Z.Š.; data curation, T.M.; writing—original draft preparation, A.M.; writing—review and editing, P.M.; visualization, A.M.; supervision, N.D.; project administration, Z.Š.; funding acquisition, Z.Š. All authors have read and agreed to the published version of the manuscript.

Funding: This work has been supported by the Scientific Grant Agency of the Ministry of Education of the Slovak Republic (Project KEGA 051ŽU-4/2025, KEGA 003TUKE-4/2024, KEGA 003EU-4/2025, VEGA 1/0609/25 and VEGA 1/0383/25).

Institutional Review Board Statement: Not applicable.

Informed Consent Statement: Not applicable.

Data Availability Statement: The original contributions presented in this study are included in the article. Further inquiries can be directed to the corresponding author.

Conflicts of Interest: Author Tomáš Mišenčík was employed by the company Iveco Czech Republic, a. s. The remaining authors declare that the research was conducted in the absence of any commercial or financial relationships that could be construed as a potential conflict of interest.

References

1. Eurostat. Population Structure and Ageing. Available online: https://ec.europa.eu/eurostat/statistics-explained/index.php?title=Population_structure_and_ageing (accessed on 20 March 2026).
2. Wang, P.; Wang, Y.; Su, P.; Wang, M.; Yang, Y.; Luo, M.; Cui, J.; He, J.; Han, L. Research and Design of Mobility Aids. *J. Phys. Conf. Ser.* **2021**, *1748*, 062054. [CrossRef]
3. Divya, R.; Murali, K.T.M.; Manuj, R.; Nithya, R. Design and Development of Mobility Aid for Physically Challenged. *Int. J. Appl. Eng. Res.* **2018**, *13*, 12522–12526.
4. Haugen, L.F. Designing for Mobility. Examining How Design Can Help Improve the Mobility and Quality of Life Among the Elderly. Available online: https://www.ntnu.edu/documents/139799/1270604448/TPD4505.Lisa.Frodadottir.Haugen.pdf (accessed on 23 July 2025).
5. Zhang, B.; Wang, Z.; Li, Z. Mobility Aid Design for the Elderly (MADE): A design thinking approach using a smart walker as a case study. *Humanit. Soc. Sci. Commun.* **2024**, *11*, 1469. [CrossRef]
6. Cao, J.; Jain, K.; Zhang, J.; Peng, Y.; Patel, S.; Mankoff, J. "A Tool for Freedom": Co-Designing Mobility Aid Improvements Using Personal Fabrication and Physical Interface Modules with Primarily Young Adults. In Proceedings of the 2025 CHI Conference on Human Factors in Computing Systems (CHI '25), Yokohama, Japan, 26 April–1 May 2025; pp. 1–16. [CrossRef]
7. Scheffers, M.F.; Ona Ayala, K.E.; Ottesen, T.D.; Tuakli-Wosornu, Y.A. Design and development of mobility equipment for persons with disabilities in low-resource and tropical settings: Bamboo wheelchairs. *Disabil. Rehabil. Assist. Technol.* **2019**, *16*, 377–383. [CrossRef] [PubMed]
8. Zhang, Y.; Tao, C.; Wang, H.; Fan, Y. Biomechanical effects of human-mobility aid interaction: A narrative review. *Gait Posture* **2025**, *118*, 1–12. [CrossRef] [PubMed]
9. Dávila-Soberón, S.; Morales-Díaz, A.; Castelán, M. A novel image dataset for detecting and classifying mobility aid users. *Expert Syst. Appl.* **2025**, *293*, 128697. [CrossRef]
10. Steyn, N.; Hamam, Y.; Monacelli, E.; Djouani, K. Modelling and design of an augmented reality differential drive mobility aid in an enabled environment. *Simul. Model. Pract. Theory* **2015**, *51*, 115–134. [CrossRef]
11. Bhuiya, M.M.R.; Hasan, M.M.U.; Shao, W. Into the Nexus of disability, mobility aid and travel Behavior—A Tale from a South Asian City. *Transp. Res. Interdiscip. Perspect.* **2024**, *28*, 101274. [CrossRef]
12. O'Brien, M.M.; Best, K.L.; Barnabe, C.; Routhier, F.; Miller, W.C.; Harpreet, R.; Manocha, K. Feasibility of an Interactive Video-Based Training Program for Learning and Reviewing Walking Aid Skills. *Arch. Phys. Med. Rehabil.* **2025**, *106*, 1703–1711. [CrossRef] [PubMed]
13. Deb, A.; Wypych, Z.; Lonner, J.; Ashrafiuon, H. Design and Control of an Autonomous Robot for Mobility-Impaired Patients. *J. Med. Robot. Res.* **2021**, *6*, 2150007. [CrossRef]
14. Zhou, Z.; Wang, L.; Dong, Y. Research on innovative design of community mutual aid elderly care service platform based on Kano model. *Heliyon* **2023**, *9*, e15546. [CrossRef] [PubMed]
15. Paetzold, K.; Wartzack, S.; Krause, D. Platform of Design Method for Developing Mobility-preserving Products. *Procedia CIRP* **2014**, *21*, 409–414. [CrossRef]
16. Mishra, R.K.; Hamad, A.; Ibrahim, R.; Mathew, M.; Talal, T.; Al-Ali, F.; Park, C.; Davuluri, V.; Fernando, M.E.; Najafi, B. Objective assessment of mobility among adults with diabetes and end-stage renal disease using walking aid: A cross-sectional cohort study. *Clin. Biomech.* **2023**, *107*, 106014. [CrossRef] [PubMed]
17. Athanasopoulou, L.; Papacharalampopoulos, A.; Stavropoulos, P.; Mourtzis, D. Design and manufacturing of a smart mobility platform's context awareness and path planning module: A PSS approach. *Procedia Manuf.* **2020**, *51*, 61–66. [CrossRef]
18. Purwar, A.; Bhargava, K.; Behan, E. A multi-functional mobility assist device for sit-to-stand motion. *Int. J. Ind. Ergon.* **2023**, *93*, 103396. [CrossRef]

19. Research Institute for Disabled Consumers (RiDC). Accessories for Getting into and Out of a Car. Available online: https://www.ridc.org.uk/features-reviews/out-and-about/car-adaptations/getting-and-out-car/accessories-getting-and-out-car/ (accessed on 23 July 2025).
20. Independent Living Centre. Independent Living Centre. Available online: https://www.independentlivingcentre.org.uk/equipment-advice/car-transfers-advice/ (accessed on 23 July 2025).
21. BraunAbility Europe AB. Turny Evo. Available online: https://www.braunability.eu/en/products/getting-seated/turny-evo/ (accessed on 20 March 2026).
22. Crowley, R.J.; Crowley, E.A. Leg lifter. U.S. Patent Application Publication. Available online: https://patentimages.storage.googleapis.com/d3/37/70/ce74916e36b30c/US20150351992A1.pdf (accessed on 20 March 2026).
23. NED Ansa Leg Lifter. Available online: https://askned.com.au/lifting-and-transferring-people/leg-lifters/leg-lifter/ (accessed on 20 March 2026).
24. Hospital Direct. Leg Lifter—Car. Available online: https://www.hospitaldirect.co.uk/product/car-leg-lifter-deluxe-wipeclean/# (accessed on 23 July 2025).
25. Tutorial Example. Available online: http://biomech.ftvs.cuni.cz/pbpk/kompendium/biomechanika/geometrie_hmotnost.php (accessed on 23 February 2017).
26. Janura, M. *Biomechanics II (Biomechanika II)*; University of Ostrava: Ostrava, Czech Republic, 2011; ISBN 978-80-7464-044-5.
27. Electromechanical Linear Actuators and Screw Supports. Available online: http://eir.lunarservers.com/ trade46/Promebat/Elektromechanische_vijzel_actuator.pdf (accessed on 21 February 2017).
28. Raeymaekers, B. *Design of Mechanical Elements—A Concise Introduction to Mechanical Design Considerations and Calculations—8.2.5 Collar Friction*; John Wiley & Sons: Hoboken, NJ, USA, 2022; p. 136. Available online: https://app.knovel.com/hotlink/pdf/id:kt013EPLUV/design-mechanical-elements/collar-friction (accessed on 28 July 2025).
29. Marrs, J. *Machine Designers Reference—11.6.1 Screw Characteristics*; Industrial Press: New York, NY, USA, 2012; p. 664. Available online: https://app.knovel.com/hotlink/pdf/id:kt0097WKX2/machine-designers-reference/screw-characteristics (accessed on 28 July 2025).
30. Roton Products, Inc. Formula Calculators. Available online: https://www.roton.com/screw-university/formula-calculators/ (accessed on 28 July 2025).
31. RoyMech. Available online: https://www.roymech.co.uk/Useful_Tables/Cams_Springs/Power_Screws_1.html (accessed on 28 July 2025).
32. The Engineering ToolBox. Screw Jack—Effort Force vs. Load. Available online: https://www.engineeringtoolbox.com/screw-jack-d_1308.html (accessed on 28 July 2025).
33. Baker, D.W.; Haynes, W. Engineering Statics Open and Interactive—9.4 Screw Threads. Available online: https://engineeringstatics.org/Chapter_09-screw-friction.html (accessed on 28 July 2025).
34. WM Berg Inc. How to Calculate Lead Screw Maximum Load, Speed & More. Available online: https://www.wmberg.com/resources/tech-and-application-support/lead-screw-load (accessed on 28 July 2025).
35. MITCalc. Power Screw. Available online: https://www.mitcalc.com/doc/powerscrew/help/en/PowerScrew.htm (accessed on 28 July 2025).